

Article

Influence of Vanadium–Titanium Sinter Basicity on Cohesive Dripping Properties of Blast Furnace Comprehensive Burden

Zhe Ning¹, Xiyu Wang¹ and Songtao Yang^{1,2,*}

¹ School of Materials and Metallurgy, University of Science and Technology Liaoning, Anshan 114051, China; classal@126.com (Z.N.); wxysd2024@163.com (X.W.)

² Key Laboratory of Liaoning Province for Recycling Science of Metallurgical Resources, Northeastern University, Shenyang 110819, China

* Correspondence: yangsongtao1984@163.com; Tel.: +86-13889856506

Abstract: Vanadium–titanium ore possesses significant mining and utilization value. The basicity of vanadium–titanium sinter has a direct impact on the formation, location, thickness, permeability, and heat exchange of the cohesive zone in the blast furnace. This paper investigated the influence of increasing the basicity of the sinter on the comprehensive burden’s cohesive dripping properties in the blast furnace, while keeping the final slag basicity constant. This study was conducted through cohesive dripping property experiments. The findings indicated that as the sinter basicity in the comprehensive burden structure increased and the corresponding increase in the proportion of pellets occurred, the softening performance of the comprehensive burden improved, the cohesive zone became thinner, the lower edge of the cohesive zone shifted upward, and the softening melting properties became better in general. With an increase in the sinter basicity, the dripping difference pressure of the comprehensive burden decreased, and the dripping rate firstly increased and then decreased. An increase in the sinter basicity of the comprehensive burden structure promoted V reduction, and the V element yield and Cr element yield of the sinter were both increased; the optimal sinter basicity was 2.5, and the corresponding pellet proportion was 42%.

Keywords: vanadium–titanium ore; cohesive dripping properties; basicity; sinter



Citation: Ning, Z.; Wang, X.; Yang, S. Influence of Vanadium–Titanium Sinter Basicity on Cohesive Dripping Properties of Blast Furnace Comprehensive Burden. *Minerals* **2024**, *14*, 293. <https://doi.org/10.3390/min14030293>

Academic Editors: Álvaro Aracena Caipa and Hyunjung Kim

Received: 1 February 2024

Revised: 4 March 2024

Accepted: 7 March 2024

Published: 11 March 2024



Copyright: © 2024 by the authors. Licensee MDPI, Basel, Switzerland. This article is an open access article distributed under the terms and conditions of the Creative Commons Attribution (CC BY) license (<https://creativecommons.org/licenses/by/4.0/>).

1. Introduction

Vanadium–titanium ore is abundant in iron, vanadium–titanium elements, and trace amounts of chromium, cobalt, and other rare metal elements, making it highly valuable for mining and utilization [1–3]. These ores are primarily found in countries such as Russia, Canada, South Africa, the United States, Brazil, and Finland. In China, they are mainly distributed in Panzhihua, Chengde, Ma’anshan, and Chaoyang in Liaoning Province, among other regions, with a wide distribution and rich reserves [4,5]. The smelting of vanadium–titanium ore is primarily carried out using the blast furnace process, which is employed by Chengde Iron & Steel, Panzhihua Iron & Steel, the Jianlong Group in China, and some steel mills in Russia [6–8]. Due to the coarse particle size of vanadium–titanium ore suitable for sintering raw materials, the current blast furnace smelting of vanadium–titanium ore comprehensive burden structure is mainly a “high basicity sinter + acidic pellet + lump ore”, and the proportion of sinter has long been maintained at more than 70% [6–8].

From the perspective of the world’s iron production practice and before the process changes, pellets replacing the sinter is the future development trend. In terms of the sintering and pelletizing processes for the production of iron-bearing raw materials, the energy consumption of the pelletizing process is less than half that of the sintering process, or even up to one third. From the point of view of the flue gas emission, it is also lowest in pelletizing, generally at 1300 m³/t, while that of the sintering ore is 4000 m³/t. The carbon emission from the pelletizing process is only 20% to 45% that of the sintering

process, and, in addition, the nitride and sulfide emissions from the sintering process are significantly higher [9]. Due to this, increasing the proportion of pellets in the blast furnace is becoming a new direction for the development of blast furnace ironmaking in China [9]. With the implementation of China's green and low-carbon manufacturing policy, and the advancement of vanadium–titanium ore grinding and beneficiation technology, the blast furnace burden structure will be oriented towards increasing the proportion of pelletized ore.

As the proportion of pellets increases, the composition of acidic materials also increases, necessitating adjustments in the material structure of the sintering process. This involves improving the basicity of vanadium–titanium sinter to ensure a reasonable control of the slag basicity. The basicity of vanadium–titanium sinter directly affects the formation, position, thickness, permeability, and heat exchange of the cohesive zone (softening zone) in the blast furnace. It also influences the formation and nature of the initial slag in the blast furnace, which in turn affects the slagging system and thermal system of the furnace [10–15].

Scholars both domestically and abroad have researched the microstructure of vanadium–titanium sinter with varying basicity and its impact on metallurgical properties [16–23]. An increase in sinter basicity leads to corresponding increases in the softening start and termination temperatures, resulting in a shorter interval for the entire softening temperature. The initial melting temperature increases, and the melting zone becomes narrower. This can be attributed to the constant SiO_2 content in the sintering process. With increased basicity, the lime dosage increases, and CaO in the sintering process is more likely to combine with TiO_2 to form perovskite. However, perovskite has a higher melting point and poor reducibility, making it difficult to be reduced during the cohesive dripping process. This has a significant impact on the cohesive dripping properties of the burden in the cohesive zone, ultimately leading to an increased differential pressure in the material column and a deterioration in the comprehensive indexes of cohesive dripping properties. Previous studies have also examined the effects of basicity on the sintering behavior and reduction process of low-titanium vanadium–titanium magnetite. The authors found that increasing the basicity (1.9–2.7) improved the reduction disintegration index and tumbler index of chromium-containing vanadium–titanium sinter [24–26]. Other studies investigated the effects of varying the basicity on the high-temperature physical properties of a vanadium–titanium-containing blast furnace burden, such as the softening temperature, melting temperature, maximum differential pressure, and softening–melting comprehensive index [27,28]. However, these studies mostly focused on sinter single burdens and neglected the interaction between different burdens in actual blast furnace conditions. As a result, they failed to clearly reflect the complete dynamic migration and transformation process of valuable metals in the comprehensive burden.

To ensure the smooth separation of slag and iron in the blast furnace, it is necessary to increase the basicity of the sinter in proportion to the increased proportion of pelletized ore in the furnace. This helps maintain a stable slag basicity in the furnace. Therefore, experiments using the new mixing calculation method for the final slag basicity as the benchmark will be the sinter and pellet proportional mix of the comprehensive burden, the cohesive dripping properties measurement furnace for comprehensive burden temperature reduction experiments, and then, to determine in the case of increasing the proportion of pellets in the case of a good blast furnace burden structure and to determine the basicity of the sinter, to provide guidance for the production practice.

2. Materials and Methods

2.1. Experimental Raw Materials

The experiments utilized iron-containing raw materials from the Chengde region. Four types of vanadium–titanium sinters, labeled A, B, C, and D, were used, each with varying basicity. Additionally, vanadium–titanium pellets from the same region were included. The chemical compositions of the sinter and pellets can be found in Table 1. The iron grade

(TFe) in the sinters exceeded 50%, and their TiO₂ content was approximately 1.8%. The binary basicity of the sinters ranged from 1.9 to 2.5. On the other hand, the pellets had an iron grade (TFe) of 60.74% and a TiO₂ content of 1.61%, with a binary basicity of 0.31. The Shenhua coke used in the experiment met the national standard GB/T 1996–2003. Its reactivity (CRI) was 25.1% and the coke strength after reaction (CSR) was 68.8%. It had a fixed carbon content of 84.98% and an ash composition, as shown in Table 2.

Table 1. Chemical composition of sinter (mass fraction, %).

Item	TFe	CaO	SiO ₂	V ₂ O ₅	Al ₂ O ₃	TiO ₂	MgO	Cr ₂ O ₃	R (CaO/SiO ₂)
Sinter A	54.17	9.84	5.17	0.27	2.06	1.86	2.66	0.22	1.9
Sinter B	53.43	10.85	5.16	0.26	2.04	1.83	2.69	0.20	2.1
Sinter C	52.69	11.87	5.16	0.26	2.02	1.81	2.72	0.21	2.3
Sinter D	51.98	12.84	5.15	0.25	2.00	1.78	2.75	0.23	2.5
Pellet	60.74	2.60	8.06	0.38	2.90	1.61	2.17	0.32	0.31

Table 2. Proximate analysis of the coke breeze and the ash composition (wt. %).

Fixed Carbon	Total Sulfur	Volatile	Ash (14.00)						Σ
			FeO	CaO	SiO ₂	MgO	Al ₂ O ₃	Others	
84.00	0.50	1.50	0.14	0.48	7.50	0.15	2.72	2.89	100.00

2.2. Experimental Equipment and Methods

To simulate the softening and dripping process of the burden in a blast furnace, the experiment utilized an iron ore high temperature cohesive dripping property determination furnace (RDL-2021; Anshan Kexiang Instrument and Meter Co., Ltd., Anshan, China) for comprehensive burden heating reduction experiments, and this device meets the requirements of the Chinese national standard GB/T 34211-2017 [29]. The device had a maximum control temperature of 1600 °C, a displacement sensor, electronic balance and differential pressure transmitter, and the equipment diagram is shown in Figure 1. In the blast furnace, the final slag binary basicity was $R = 1.10$, with a coke ratio of 350 kg/t, coke butyl ratio of 20 kg/t, and coal ratio of 160 kg/t, all of which remained unchanged. The study focused on the sinter basicity and the proportion of the pellets added to the furnace to investigate the cohesive dripping properties of the comprehensive burden. The heating procedure is presented in Table 3.

Table 3. Testing programs of BF burden for cohesive dripping properties (%).

Item	Comprehensive Burden Ratio/%	Basicity of Sinter (R = CaO/SiO ₂)	Estimated Basicity of Blast Furnace Final Slag (R = CaO/SiO ₂)
1	Sinter A (75%) + Pellet (25%)	1.9	1.1
2	Sinter B (69%) + Pellet (31%)	2.1	1.1
3	Sinter C (63%) + Pellet (37%)	2.3	1.1
4	Sinter D (58%) + Pellet (42%)	2.5	1.1

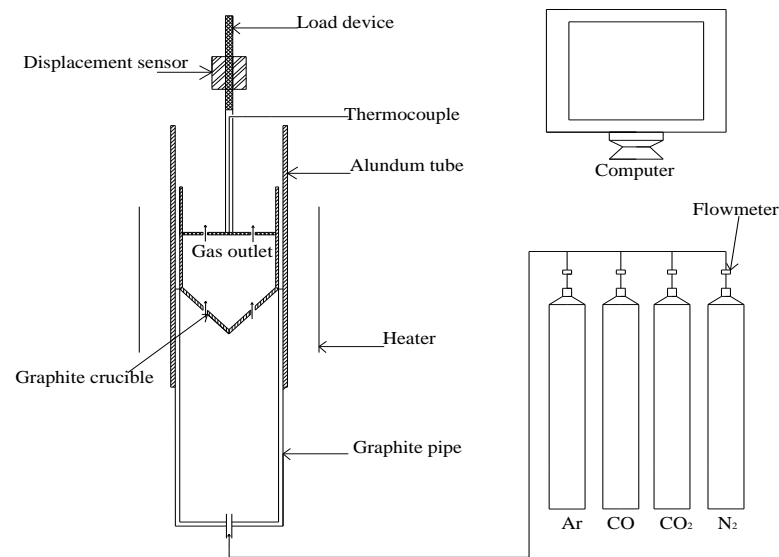


Figure 1. The softening–melting property experiments.

A graphite crucible was used in the experiment with the following dimensions: inner diameter $\Phi 75$ mm, inner height 160 mm, and bottom hole diameter $\Phi 10$ mm. To simulate the laminar distribution of blast furnace ore and coke, the lower layer of the graphite crucible was loaded with 30 mm of coke, approximately 73.5 g. Then, 500 g of the comprehensive burden was placed in the middle layer of the crucible, with a height of approximately 70 mm. The upper part was similarly spread with 15 mm thick coke particles, approximately 36.5 g. The temperature was raised to approximately 2.5 °C. The heating and gas distribution system is shown in Table 4. N₂ was passed in during the experiment to protect the raw materials from oxidation. The experiment was conducted with a heating rate of 10 °C/min from 0 to 900 °C, 3 °C/min from 900 to 1020 °C, and 5 °C/min at 1020 °C. A displacement sensor (range ≥ 100 mm, resolution ≤ 0.1 mm) was used to monitor the change of the layer height in real time and to calculate the shrinkage rate at the same time; an electronic balance (range 30 kg, accuracy 0.10 g) was used to monitor the change of weight loss in the experimental process; and a differential pressure transmitter (range ≥ 50 kPa, accuracy $\leq 0.25\%$ F.S.) was used to monitor the difference of the pressure between the air inlet and the air outlet. The pressure difference between inlet and outlet was monitored using a differential pressure transmitter (range ≥ 50 kPa, accuracy $\leq 0.25\%$ F.S.). The experiment was concluded when the shrinkage rate of the specimen no longer demonstrated significant changes. At the end of the experiment, the reducing gas was replaced by N₂ to protect the specimen during cooling to room temperature. Subsequently, the specimen was removed for analysis. Following the primary slag generation experiment, the residue in the crucible was removed and separated to obtain the residual slag sample (Ar). For the same specimen, there were at least 2 measurements. For the same specimen, the experimental results were in accordance with the provisions of Appendix B of the Chinese national standard GB/T 34211-2017. If the difference between the two test results of the same specimen was within the range, the test was qualified.

Table 4. Experimental conditions for carrying out softening and melting tests.

Temperature Range	0~400 °C	400~900 °C	900~1020 °C	1020 °C~Dripping Temperature
Gas composition	N ₂ 100% 3 L/min	N ₂ 60% 9 L/min CO 26% 3.9 L/min CO ₂ 14% 2.1 L/min	N ₂ 70% 10.5 L/min CO 30% 4.5 L/min	
Furnace ramping rate	10 °C/min	10 °C/min	3 °C/min	5 °C/min

The experiment examined various properties parameters, such as the softening zone (ΔT_1), melting zone (ΔT_{DS}), and temperature interval of the cohesive zone (ΔT_{D1}) of the burden, as well as permeability. The softening start temperature T_{10} was the temperature when the shrinkage rate was 10%, and the softening end temperature T_{40} was the temperature when the shrinkage rate was 40%. The melting start temperature T_S was the temperature at which the differential pressure rose most violently, which is also known as the differential pressure steep rise temperature. In this experiment, the differential pressure rises to 400 Pa as the differential pressure has a steep rise state, the melting end temperature T_D is the temperature at which the dripping begins, and the maximum differential pressure ΔP_{max} corresponds to the highest differential pressure peak that occurs in the course of the experiment on the ore material. These parameters were calculated based on Equations (1)–(3), respectively:

$$\Delta T_1 = (T_{40} - T_{10}) \quad (1)$$

$$\Delta T_{DS} = (T_D - T_S) \quad (2)$$

$$\Delta T_{D1} = (T_D - T_{10}) \quad (3)$$

The total eigenvalue, S , represents the piezoresistive load that the blast furnace is subjected to during the smelting of the ore softening and dripping. Similar to the maximum differential pressure, a smaller value of S indicates better dripping properties. The calculation process follows the formula

$$S = \int_{T_S}^{T_D} (P_m - \Delta P_S) \bullet dT \quad (4)$$

where T_D denotes the beginning of the dripping temperature in degrees Celsius, T_S represents the beginning of the melting temperature in degrees Celsius, P_m refers to any temperature T when the differential pressure is measured in Pascals, and ΔP_S indicates the beginning of the melt when the differential pressure is measured in Pascals.

The microstructure of the slag samples was observed using a Zeiss polarizing microscope (Cambridge Q500; Leica Microsystems; Wetzlar, Germany) and an S-3400N scanning electron microscope (JEOL Ltd., Tokyo, Japan). The chemical composition of the raw materials and post-experimental samples was determined using an X-ray fluorescence spectrometer (XRF) (PANalytical Axios; MalvernPanalytical; Almelo, The Netherlands) using the X-fluorescence full-scan rapid analysis method. The test procedure was as follows: (1) grind the sample to be measured into a fine powder; (2) press the sample powder into thin slices with a tablet press; (3) place the prepared sample slices into the sample tray of the XRF spectrometer and set the instrument parameters, such as voltage, current, time, etc.; (4) turn on the instrument and start the measurement (the instrument will automatically record the characteristic X-ray wavelengths and intensities of the samples); (5) the instrument automatically converts elemental contents based on the elemental spectral line intensities. The instrument automatically converts the elemental content.

3. Results

3.1. Softening Properties

Figure 2 presents a schematic diagram of the softening properties of the comprehensive burden with different sinter basicity values. It can be observed that as the sinter basicity and pellet proportion increased, there was not much change in the softening start temperature of the comprehensive burden, but the softening end temperature decreased, with T_{40} ranging from 1310.5 °C to 1276.8 °C, and the softening zone became narrower, with ΔT_1 decreasing from 154.9 °C to 117.9 °C.

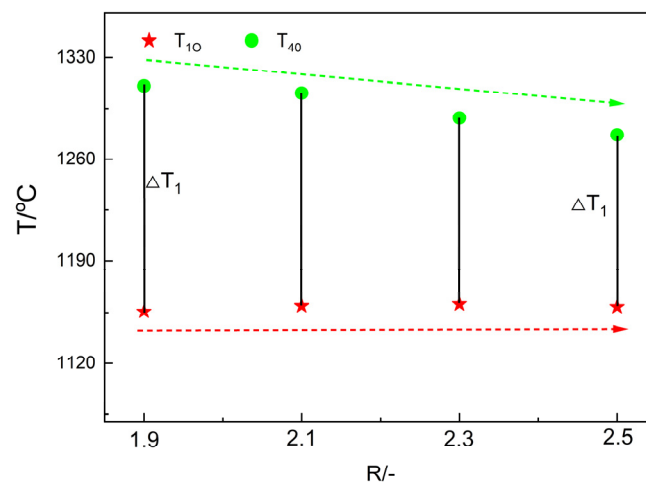


Figure 2. Effects of sinter basicity on T_{10} , T_{40} and softening zone.

3.2. Melting Properties

Figure 3 illustrates the impact of sinter basicity on the soft melting and the dripping properties of the comprehensive burden. With an increase in the sinter basicity and the proportion of pelletized ore in the furnace, both the melting start and end temperatures of the comprehensive burden decreased, with T_S ranging from 1248.9 °C to 1226.2 °C, and T_D ranging from 1408.8 °C to 1370.8 °C. However, the decrease in the melting end temperature was more significant, resulting in a narrower melting zone, with ΔT_{DS} decreasing from 159.9 °C to 144.6 °C.

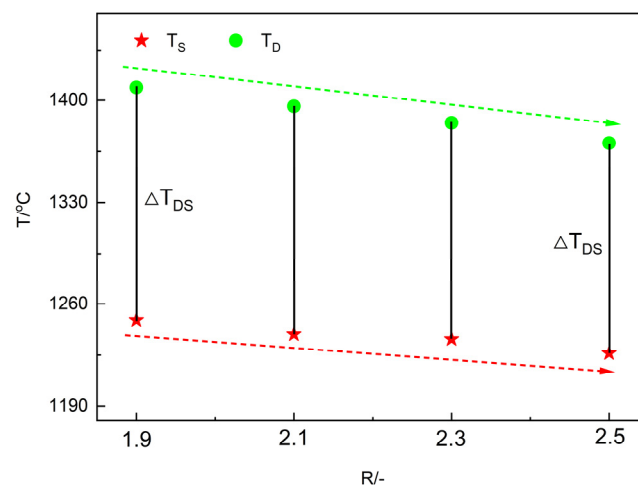


Figure 3. Effects of sinter basicity on T_S , T_D , and melting zone.

3.3. Cohesive Zone and Permeability

Figure 4 indicates the effect of the sinter basicity on the cohesive zone of the comprehensive burden. The cohesive zone is located in the middle of the blast furnace body, also known as the softening–melting zone. The cohesive zone is the area where the physico-chemical properties of the charge are converted from solid to liquid, and it is one of the most important thermo-chemical reaction zones in the blast furnace. In the cohesive zone, iron ore, flux, and coke begin to soften and melt, producing liquid iron and slag. With an increase in the sinter basicity and the proportion of pellets in the furnace, the cohesive zone of the comprehensive burden became narrower, but the lower edge of the cohesive zone moved upwards. Pellets play a crucial role in improving the permeability of the comprehensive burden. In the blast furnace smelting process, it is desirable for the burden to melt rapidly at high temperatures, as this promotes the thinning of the soft melt layer and

enhances its permeability. Therefore, an increase in the sinter basicity generally improves the soft melt properties of the comprehensive burden. Figure 5 demonstrates the impact of the sinter basicity on the permeability of the comprehensive burden. As depicted, with an increase in the sinter basicity and the proportion of pellets in the furnace, the S value and ΔP_{max} initially decreased gradually and then increased. The increase in the sinter basicity improved the sinter permeability and overall burden permeability, which contributed to the smooth operation of the blast furnace. However, as the pellets will generate a large amount of FeO through reduction at lower temperatures, the generated FeO and SiO₂ will generate substances such as 2FeO-SiO₂ with a low melting point, which melts earlier, and compromises the permeability of the burden. Therefore, an excessive proportion of pellets is unfavorable for the permeability of the comprehensive burden.

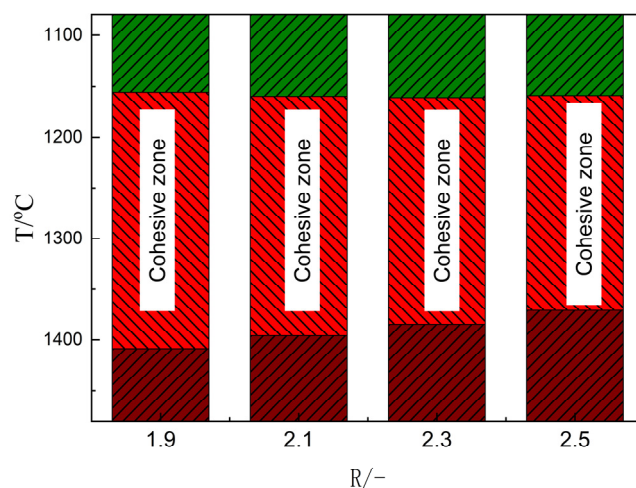


Figure 4. Effects of sinter basicity on the location of cohesive zone.

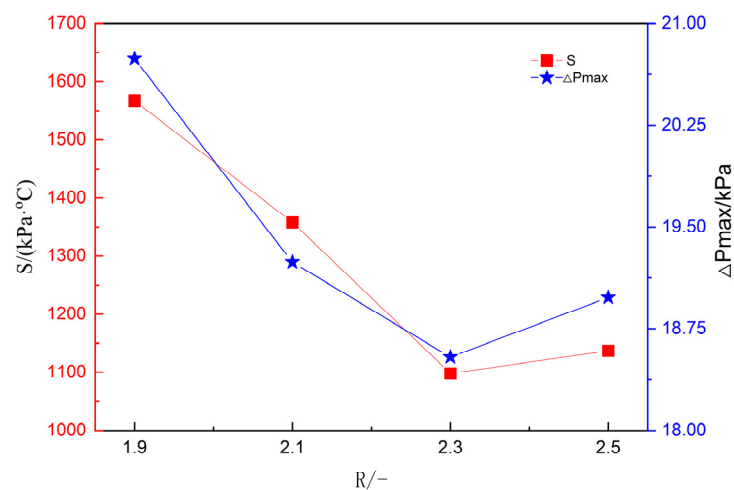


Figure 5. Permeability at different sinter basicity values.

3.4. Dripping Properties

Figure 6 depicts the impact of different sinter basicity values on the dripping properties of the comprehensive burden. With an increase in the sinter basicity and the proportion of pellets in the furnace, the dripping differential pressure of the comprehensive burden decreased, while the dripping rate initially increased and then decreased. The improved reducing property of the comprehensive burden led to a gradual enhancement in the dripping rate. However, when the sinter basicity was further increased from 2.3 to 2.5, the formation of high-melting-point compounds such as dicalcium silicate and perovskite in

the slag can result in non-homogeneous phases, affecting the viscosity of the slag phase and causing a slight decrease in the dripping rate.

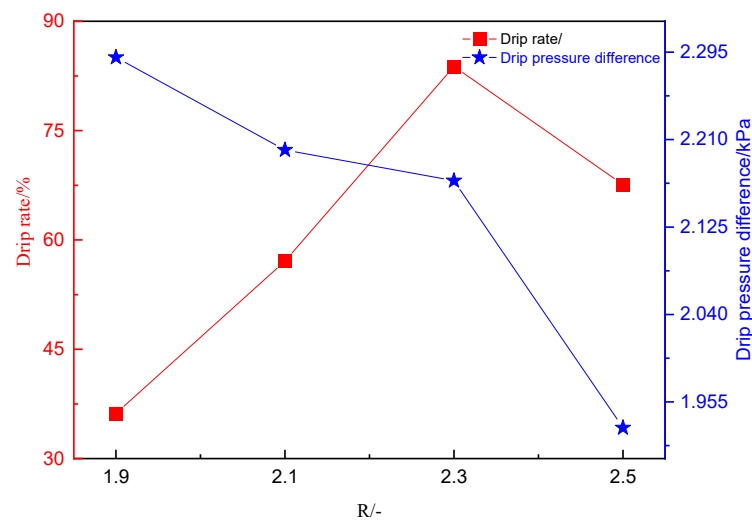


Figure 6. Dripping characteristics at different sinter basicity values.

3.5. Effect of Sinter Basicity on V and Cr Migration

Table 5 presents the composition of the slag and liquid iron after slag–iron separation. With an increase in the sinter basicity of the comprehensive burden, the content of V and Cr elements in the dripping molten iron increased. The V elemental yield rose from 40.84% to 44.54%, and the Cr elemental yield increased from 32.15% to 50.50%. Blast furnace slag is divided into primary slag, medium-term slag, and final slag. Although the slag in Table 5 was one of the final samples obtained in this experiment, it was not the final slag of the blast furnace, because the experiment did not simulate the subsequent reaction process, and there are coke direct reduction and coal injection processes in the actual production, so the slag obtained in this experiment was the medium-term slag of the blast furnace, and its composition coincided with the experimental design scheme.

Table 5. Contents of V and Cr in the dripped liquid iron and slag (mass fraction, %).

Item	Liquid Iron Composition/%								V Element Yield	Cr Element Yield
	Fe	V	Cr	Si	Mn	P	S	Ti		
1	95.89	0.209	0.061	0.16	0.37	0.12	0.05	0.22	40.84	32.15
2	96.57	0.211	0.065	0.15	0.36	0.12	0.05	0.18	41.19	34.26
3	96.61	0.222	0.087	0.15	0.32	0.11	0.06	0.19	42.29	45.86
4	96.69	0.234	0.096	0.15	0.32	0.10	0.05	0.20	44.54	50.60

Item	Slag Composition/%							
	Fe	V ₂ O ₅	Cr ₂ O ₃	CaO	SiO ₂	MgO	Al ₂ O ₃	TiO ₂
1	1.638	0.095	0.001	33.69	27.31	11.75	7.73	8.56
2	1.570	0.104	0.003	33.49	27.57	12.52	6.23	8.62
3	2.121	0.126	0.001	33.37	27.56	13.10	6.68	8.65
4	1.891	0.103	0.004	34.76	27.82	12.45	6.89	8.41

4. Discussion

When a burden is introduced into a blast furnace, it undergoes a gradual reduction from the outside to the inside in the lower, high-temperature section. A metal shell is formed on the surface of the particles through reduction, while the inner part consists of unreacted slag phase, faujasite, and a portion of silicate glass. The soft melting and dripping

behaviors of the burden are determined by the soft melting behavior of the metallic iron shell on the particle surface and the minerals in the unreacted core.

As the lower burden goes through increasing temperatures and the gas flow facilitates mass and heat transfer, the slag phase in the unreacted core begins to melt and penetrate outward. When passing through the external iron shell, the iron-containing burden contracts significantly, resulting in decreased porosity and increased differential pressure. As the temperature reaches a certain point, the melting point of metallic iron decreases due to carburization, leading to its melting. At the same time, the slag phase also melts, creating an appropriate viscosity and better flow conditions for slag-iron dripping. In this study, the experimental results were analyzed and compared regarding softening, melting, dripping, and permeability. Compared with the cohesive characteristics of ordinary iron ores, vanadium–titanium ore has a lower softening start temperature, a wider softening zone, a lower melting start temperature, and a wider melting zone [30,31]. The reason for this is that vanadium–titanium ore has a relatively low content of faujasite in the slag and a significantly higher content of yellow feldspar and perovskite during the temperature-raising reduction process.

The softening temperature and melting temperature of the comprehensive burden mainly depend on the melting point of the low-melting-point slag phase generated during the reduction process, while ordinary iron ore depends largely on the influence of iron-containing oxides, i.e., the degree of reduction of iron, while vanadium–titanium ores sintered during the process due to TiO_2 are easy to combine with CaO to form a high melting point of the mineral perovskite and inhibit the formation of calcium ferrite. The vanadium–titanium sinter in the content of calcium ferrite is significantly lower than that of titanium-free sinter, so the softening and melting temperatures of the vanadium–titanium comprehensive burden are affected by the multiple effects of the iron-containing oxides and titanium-containing oxides. With the other conditions basically unchanged, when the CaO content in the comprehensive burden increased, it was easier to generate a slag phase with a lower melting point under high temperature reduction, such as calcium iron olivine, etc. Therefore, when the CaO content was higher, the softening start temperature of the comprehensive burden was relatively low, but since the softening start temperature of the pellet was lower than that of the sinter with the same chemical composition, the softening start temperature would be basically the same when the chemical composition in the comprehensive burden was basically the same.

An increase in the sinter basicity raises the melting start and end temperatures of the sinter, primarily due to the increased CaO content, resulting from the higher sinter basicity. This elevation in the CaO content leads to an increase in high melting point substances such as CaO-TiO_2 , titanium garnet, and 2CaO-SiO_2 in the sinter, thereby increasing its melting temperature. However, the increase in sinter basicity also raises the proportion of pellets, which have a narrower cohesive zone. Consequently, the comprehensive burden exhibits a narrower cohesive zone and an upwards shift of the entire melting temperature zone within the blast furnace. For efficient blast furnace operation, it is advantageous to have a higher melting start temperature and a narrower melting temperature interval, as well as a soft melting belt positioned slightly lower and a dripping temperature that is not excessively high. These factors contribute to favorable gas flow towards the downstream burden in ironmaking operations.

Figure 7 displays the typical microstructures of the dripping slag observed at the end of the soft-melt dripping experiments for the four burdens of vanadium–titanium magnetite. There were no significant differences in the microstructures of the slag from the four experiments. The structure was complex and mainly composed of perovskite, yellow feldspar, calcium silicate, and vitreous materials. Perovskite was mainly embedded in the yellow feldspar in two forms: sheet-like compact structures and cross-shaped, long-grained hollow structures. There was also a small amount of calcium silicate and vitreous embedded in the yellow feldspar. The slag from schemes 1 and 2 of the lower basicity sinters contained a noticeable number of metallic iron particles, mainly due to their higher

titanium content, which generated more TiC encapsulating the metallic iron and affected the dripping behavior.

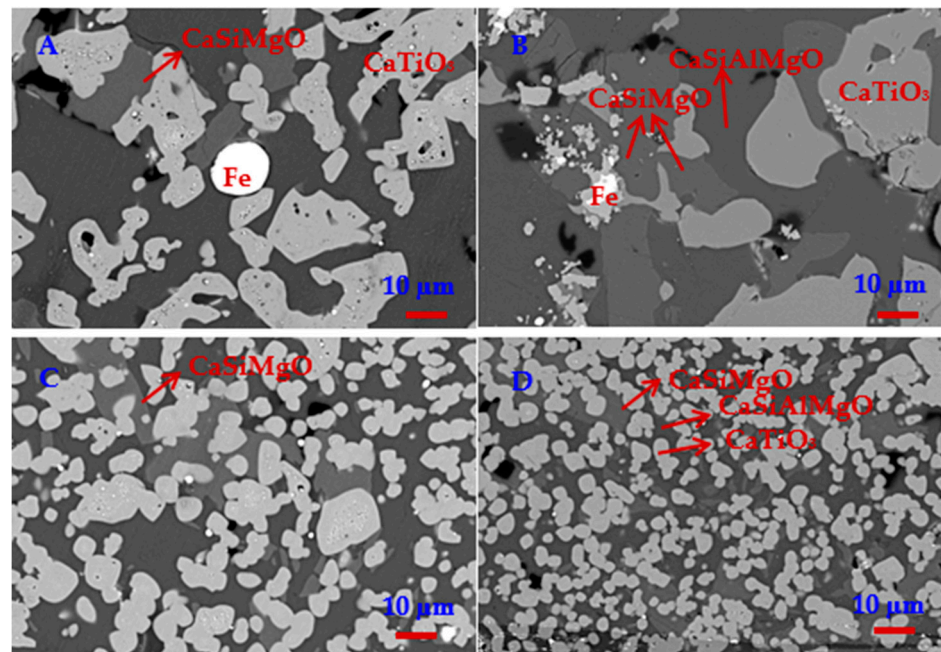


Figure 7. Microstructure of slag samples at the end of the experiment: (A) $R = 1.9$; (B) $R = 2.1$; (C) $R = 2.3$; (D) $R = 2.5$.

The material that successfully dripped included an Fe_3C phase and an α -iron phase, while the non-dripped material was composed of metallic iron, iron vanadium–chromium aggregates, and carbon (C). The vanadium–chromium aggregates were unevenly distributed in the metallic iron, and carbon was embedded in the metallic iron in the form of lines. These unreacted carbon strips increased the viscosity and reduced the mobility of the molten iron, resulting in the lack of dripping under the experimental conditions and timeframe. Consequently, the yield of Fe, V, and Cr elements was low, especially due to the presence of Fe-V-Cr aggregates in the non-dripped material, which reduced the vanadium and chromium yield to less than 50%. With an increase in the sinter basicity in the comprehensive burden, the content of V and Cr elements in the dripping iron increased, and their yields also rose. The increase in sinter basicity resulted in higher concentrations of hematite and calcium ferrite, which exhibited better reducing properties, and a decrease in magnetite, which has a poorer reducing property. Thus, the reducing properties of the sinter were improved. Additionally, the increase in the amount of melt led to a greater contraction in the sintered layer, promoting higher sinter porosity and enhancing internal diffusion during the iron ore reduction. This improvement in the sinter reducing properties facilitates the reduction of V and Cr. Furthermore, the increase in sinter basicity elevates the CaO content, which improves the conditions for silicon reduction of vanadium oxides, thereby promoting vanadium reduction by silicon.

In conclusion, it is evident that increasing the sinter basicity in the comprehensive burden is favorable for the reduction of the elements V and Cr.

5. Conclusions

The study yielded several key findings:

- (1) Compared with the cohesive characteristics of ordinary iron ores, vanadium–titanium ore has a lower softening start temperature, a wider softening zone, a lower melting start temperature, and a wider melting zone.

- (2) With the increase of sinter basicity in the comprehensive burden structure and the corresponding increase of the proportion of pellets in the comprehensive burden structure, the softening zone became narrower, and the softening performance was improved; the melting zone was obviously narrowed, and the melting temperature zone shifted upwards within the blast furnace; the cohesive zone became thinner, the lower edge of the cohesive zone shifted upwards, and the whole cohesive zone shifted upwards within the blast furnace.
- (3) The sinter basicity in the comprehensive burden structure increased from 1.9 to 2.5, the permeability increased and then decreased, the dripping rate first increased and then decreased, and the V and Cr yield reduced as the sinter basicity increased.
- (4) Based on the softening, melting, and dripping properties of the comprehensive burden, the optimum basicity of sinter is 2.5 under the experimental conditions used, and the corresponding pellet ratio is less than 42%.

Author Contributions: Z.N. and S.Y. contributed to the material synthesis, and performed the experiments, material characterization, data analysis, and paper writing; X.W. revised the paper and refined the language; S.Y. contributed to the design of the experiment. All authors have read and agreed to the published version of the manuscript.

Funding: This research was financially supported by the Programs of the National Natural Science Foundation of China (No. 52174319).

Data Availability Statement: The data presented in this study are available on request from the corresponding author due to privacy.

Conflicts of Interest: The authors declare no conflicts of interest.

References

1. Rogers, D.B.; Arnott, R.J.; Word, A.; Goodenough, J.B. The preparation and properties of some vanadium spinels. *J. Phys. Chem. Solids* **1963**, *24*, 347–360. [[CrossRef](#)]
2. Guo, X.C. Utilization status and use value of vanadium titanium magnetite. *Panzhuhua Sci. Technol.* **1996**, *2*, 14–18.
3. Peng, Y.J.; Lv, C. Current situation and progress of comprehensive utilization of vanadium titanium magnetite. *Min. Res. Dev.* **2019**, *39*, 130–135.
4. Xue, X.; Wu, D.H. Different technological processes and evaluation of comprehensive utilization of vanadium titanium magnetite. *China Metallurgy*. **2012**, *22*, 22–26.
5. Chu, M.S.; Tang, J.; Liu, Z.G. Current situation and progress of comprehensive utilization of high chromium vanadium titanium magnetite. *J. Iron Steel Res.* **2017**, *29*, 335–344.
6. Yang, J.; Jiang, T.; Ma, S.H.; Yang, S.T.; Zhou, M. Kinetics and mechanism of coal-based direct reduction of highchromium vanadium-titanium magnetite. *J. Iron Steel Res. Int.* **2022**, *29*, 11. [[CrossRef](#)]
7. Chen, B.; Jiang, T.; Wen, J.; Li, L.; Zhu, F.; Hu, P.; Rao, J. Reducibility optimization and reaction mechanism of high-chromium vanadium-titanium magnetite flux pellets. *Metall. Mater. Trans. B. Process Metall. Mater. Process. Sci.* **2023**, *5*, 2503–2518. [[CrossRef](#)]
8. Qin, J.; Liu, G.G.; Li, Z.J. Review of several typical processes for direct reduction treatment of vanadium titanate resources. *Min. Metall.* **2014**, *23*, 79–82+91.
9. Jin, Y.L.; He, Z.J.; Wang, C. Analysis on low carbon emission of blast furnace with different raw materials structure. *Iron Steel* **2019**, *54*, 8–16.
10. Song, G.C.; Wan, T.Y.; Chen, X.X. Study on the phase composition of the soft melting dropping zone of vanadium titanium sinter in blast furnace smelting. *Iron Steel Vanadium Titan.* **1996**, *17*, 3.
11. Park, H.; Park, J.Y.; Kim, G.H.; Sohn, I. Effect of TiO₂ on the viscosity and slag structure in blast furnace type slags. *Steel Res. Int.* **2012**, *83*, 150–156. [[CrossRef](#)]
12. Zhou, K. Research on the Soft Melting Properties and Phase Change Law of Vanadium Titanium Furnace Charge. Ph.D. Thesis, Chongqing University, Chongqing, China, 2020.
13. Zhao, W.; Chu, M.S.; Guo, H.W.; Liu, Z.G.; Yan, B.J.; Li, P. Interface behavior and interaction mechanism between vanadium-titanium magnetite carbon composite briquette and sinter in softening-melting-dripping process. *ISIJ Int.* **2020**, *61*, 146–157. [[CrossRef](#)]
14. Liu, H.; Zhang, K.; Ling, Q.; Qing, Y.L. Effect of B₂O₃ content on the sintering basic characteristics of mixed ore powder of vanadium-titanium magnetite and hematite. *J. Chem.* **2020**, *7*, 6279176. [[CrossRef](#)]
15. Du, H.G. *Principle of Smelting Vanadium-Titanium Magnetite in the Blast Furnace*; China Science Publishing & Media Ltd.: Beijing, China, 1996; pp. 1–3.

16. Lin, W.K.; Hu, P. Study on the Influence of TiO₂ content and basicity level on the metallogenic law of vanadium titanium sinters. *Iron Steel Vanadium Titanium*. **2020**, *41*, 94–100.
17. Cheng, G.; Gao, Z.; Yang, H.; Xue, X. Effect of Calcium Oxide on the Crushing Strength, Reduction, and Smelting Performance of High-Chromium Vanadium–Titanium Magnetite Pellets. *Metals*. **2017**, *7*, 181. [[CrossRef](#)]
18. Gan, Q.; He, Q.; Li, J.M. The effect of SiO₂/TiO₂ ratio and auxiliary materials on the soft melt dripping properties of vanadium titanium sinter. *Iron Steel*. **2000**, *4*, 1–4.
19. Paananen, T.; Kinnunen, K. Effect of TiO₂-content on reduction of iron ore agglomerates. *Steel Res. Int.* **2009**, *80*, 408–414.
20. Fang, H.X.; Li, H.Y.; Zhang, T. Influence of CaO on existence form of vanadium-containing phase in vanadium slag. *ISIJ Int.* **2015**, *55*, 200–206. [[CrossRef](#)]
21. Wang, F.J.; Lv, Q.; Chen, S.J. The effect of TiO₂/SiO₂ on the droplet properties of vanadium titanium bearing blast furnace burden. *Iron Steel Vanadium Titan.* **2015**, *36*, 79–83.
22. Wang, H.T.; Zhao, W.; Chu, M.S. Effect and function mechanism of sinter basicity on softening-melting behaviors of mixed burden made from chromium-bearing vanadium–titanium magnetite. *J. Cent. South Univ.* **2017**, *24*, 39–47. [[CrossRef](#)]
23. Liao, J.L.; Li, J.; Wang, X.D.; Zhang, Z.T. Influence of TiO₂ and basicity on viscosity of Ti bearing slag. *Ironmak. Steelmak.* **2014**, *39*, 133–139. [[CrossRef](#)]
24. Yang, S.T.; Zhou, M.; Jiang, T.; Wang, Y.J.; Xue, X.X. Effect of basicity on sintering behavior of low-titanium vanadium–titanium magnetite. *Trans. Nonferrous Met. Soc. China* **2015**, *25*, 2087–2094. [[CrossRef](#)]
25. Yang, S.T.; Zhou, M.; Jiang, T.; Xue, X.X. Effects of dolomite on mineral compositions and metallurgical properties of chromium-bearing vanadium–titanium magnetite sinter. *Minerals* **2017**, *7*, 210. [[CrossRef](#)]
26. Tang, W.D.; Xue, X.X.; Yang, S.T. Influence of basicity and temperature on bonding phase strength, microstructure, and mineralogy of high-chromium vanadium–titanium magnetite. *Int. J. Miner. Metall. Mater.* **2018**, *25*, 871–880. [[CrossRef](#)]
27. Wang, F.J.; Lv, Q.; Chen, S.J.; Liu, R.; Li, F.G. The effect of basicity on the droplet properties of vanadium titanium bearing blast furnace burden. *Iron Steel Vanadium Titan.* **2015**, *36*, 92–96.
28. Chen, L.J.; Chu, M.S.; Liu, Z.G. The effect of flux content in vanadium titanium sinter on the reasonable burden structure of blast Furnace. In Proceedings of the 2014 National Ironmaking Production Technology Conference and Ironmaking Academic Annual Conference (Part 1), Zhengzhou, China, 13–16 May 2014.
29. GB/T 34211-2017; Iron Ores-Method for Determination of Iron Reduction Softening Dripping Performance under Load. National Standardization Administration: Beijing, China, 2017.
30. Agrawal, A. Blast furnace performance under varying pellet proportion. *Trans. Indian Inst. Met.* **2019**, *72*, 777. [[CrossRef](#)]
31. Hoque, M.M.; Doostmohammadi, H.; Mitra, S.; O’Dea, D.; Liu, X.; Honeyands, T. High temperature softening and melting interactions between Newman blend lump and sinter. *ISIJ Int.* **2021**, *61*, 2944–2952. [[CrossRef](#)]

Disclaimer/Publisher’s Note: The statements, opinions and data contained in all publications are solely those of the individual author(s) and contributor(s) and not of MDPI and/or the editor(s). MDPI and/or the editor(s) disclaim responsibility for any injury to people or property resulting from any ideas, methods, instructions or products referred to in the content.